Spatial AI:
A Unified Framework for Coherent Intelligent Environments

OCTA Research Monograph

Version 0.5 – Deep Foundations

OCTA Research

January 2026

Abstract

This monograph presents a unified geometric, physical, probabilistic, and topological framework for *Spatial AI*: a paradigm in which intelligence becomes a coherent field property of the environment itself rather than a property of embedded devices alone.

We integrate five pillars: Perfect Coherence Architecture (PCA), Perfect Attractor Geometry, Tessellated Field Synthesis (TFS), Whisper Graph Communication (WGC), and the Lattice of Computable Fields (LCF). Together these define an intelligence stack spanning field sensing, coherence generation, attractor-driven stabilization, programmable transport tensors, probabilistic whisper-based communication, and topologically robust computation.

Beyond introducing these ingredients in isolation, we show how they assemble into a closed cyber–physical loop: perception becomes a field, coherence is treated as a primary state variable, attractors stabilize macroscopic identity, TFS shapes the transport geometry of matter, WGC supports low-energy belief propagation over device graphs, and LCF provides a discrete yet topologically protected logic layer that orchestrates global modes of operation. The result is an environment that is both physically grounded and computationally expressive.

In this extended version we deepen the mathematics of coherence, develop spectral, information-theoretic, and control-theoretic views of Spatial AI, add explicit examples, and introduce additional TikZ visualizations of the architecture, TFS microstructures, WGC whisper graphs, and LCF lattices.

Contents

1 Introduction and Motivation **6**

1.1 Design Principles 6

1.2 High-Level Spatial AI Map (TikZ) 7

2 Notation and Conventions **7**

3 Perception Fields and State Geometry **8**

4 Coherence Axes **9**

4.1 Structural Coherence 9

4.2 Dynamic Coherence 9

4.3 Intent Coherence 10

4.4 Unified Coherence Index 10

5 Perfect Attractor Geometry **10**

5.1 Visualizing the Attractor Field 11

6 Attractor–Driven Dynamics and Stability **11**

7 Oscillator Networks and Synchronization **12**

8 Tessellated Field Synthesis (TFS) **12**

8.1 Domain and Mechanical Fields 12

8.2 Constitutive Coupling 13

8.3 Transport and Wave Equations 13

8.4 Metric Interpretation 14

8.5 Tessellations 14

8.6 Writing Eigenstrain 14

9 Whisper Graph Communication (WGC) **15**

9.1 Gaussian Beliefs on a Graph 15

9.2 Whisper Update Rule 16

9.3 Whisper Graph as a Stochastic Kernel . . . 16
9.4 Information-Theoretic Whisper Coherence . . . 17
9.5 Whisper Graph TikZ Diagram . . . 18
9.6 Integration of WGC with Coherence and Attractors . . . 18

10 Homogenization Theory for TFS **18**

11 Inverse Design and Optimization **19**
11.1 Protected Region Example . . . 19
11.2 Simulation Pipeline . . . 19

12 Lattice of Computable Fields (LCF) **20**
12.1 LCF as a Lattice (TikZ Hasse Diagram) . . . 21

13 Spatial AI as Unified System **21**

14 Closed–Loop Diagram **21**

15 Lyapunov Stability and Identity Attractors **21**

16 Spectral Phase Transitions in Coherence **23**

17 Information–Theoretic Coherence **23**

18 Multiscale Coherence Formalism **24**

19 Engineering Stack Architecture **25**

20 Comparative Taxonomy of Architectures **25**

21 Design Patterns and Reference Architectures **25**
21.1 Quiet Room Pattern . . . 25
21.2 Adaptive Corridor Pattern . . . 26
21.3 Vehicle Cabin Pattern . . . 27

22 Implementation Considerations **27**

22.1 Sensing and Bandwidth 27

22.2 Computation and Deployment 28

22.3 Privacy and Observability 28

23 Use-Case Scenarios **28**

23.1 Spatial AI Room 28

23.2 Spatial AI Factory Cell 29

23.3 Spatial AI Vehicle Cabin 29

24 Ethics, Safety, and Governance **30**

25 Roadmap **30**

26 Conclusion **30**

A.1Appendix A: Mathematical Foundations and Proofs **31**

A.1.1Structural Coherence as Dirichlet Energy 31

A.1.2Coherence Index as Order Parameter 31

A.2Appendix B: Spectral Coherence Thresholds **31**

A.3Appendix C: Kuramoto–Attractor Hybrid Analysis **32**

A.4Appendix D: Mechanics of TFS Eigenstrain Routing **32**

A.5Appendix E: Numerical Schemes **33**

A.5.1Finite Element Solution Strategy 33

A.5.2Topology Optimization Loop 33

A.6Appendix F: Lattice of Computable Fields (LCF) **34**

A.7Appendix G: Toy 1D Spatial AI Model **34**

A.8Appendix H: WGC Noise Floor and Spectral Gap **35**

A.9 Appendix I: Example Scales and Parameters **35**

A.10 Glossary of Key Terms **35**

A.11 References **36**

1 Introduction and Motivation

Traditional AI lives inside discrete computational units: servers, phones, vehicle ECUs, and robots. The environment is treated as a passive backdrop, instrumented at best with a thin layer of sensors and actuators.

Spatial AI reverses this perspective: the environment itself becomes a coherent, memory-bearing, anomaly-aware, computational medium. Physical space, material structures, and field configurations are elevated from *context* to *substrate*.

We consider environments such as rooms, buildings, factories, vehicles, ships, or cities. Each environment:

- senses itself through multimodal perception fields,
- forms a stable identity through coherence,
- routes energy and information through programmed transport geometries,
- communicates via whisper-like stochastic exchanges over device graphs,
- and computes by manipulating field overlaps and topology.

A Spatial AI environment is thus a distributed intelligent agent in its own right, with internal state, attractors, and policies, yet implemented as geometry-plus-fields instead of only code-plus-processors.

1.1 Design Principles

Spatial AI is built on three core principles:

P1 Field-first: represent sensing, context, and actuation as spatial fields over X, not just as device-centric signals.

P2 Coherence-first: treat coherence—structural, dynamic, and intent—as a primary design variable and control target.

P3 Topology-aware logic: implement high-level modes, safety, and invariants as topological constraints on a lattice of computable fields, rather than ad hoc procedural code.

1.2 High-Level Spatial AI Map (TikZ)

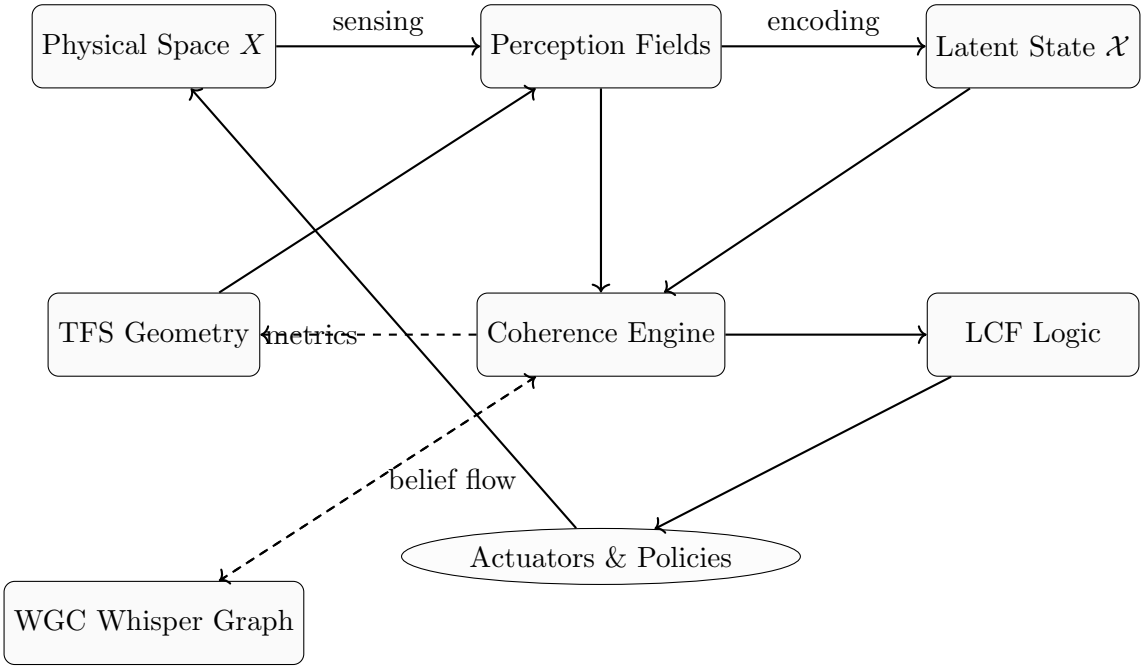

Figure 1: High-level map of Spatial AI: environment, fields, coherence engine, TFS geometry, WGC whisper graph, LCF logic, and actuation form a closed-loop system.

2 Notation and Conventions

We briefly summarize notation used throughout.

- $X \subset \mathbb{R}^d$: physical space of the environment.
- $\Omega \subset \mathbb{R}^3$: solid body for TFS mechanics.
- $G = (V, E)$: graph capturing structural or communication couplings.
- $\phi : X \times \mathbb{R}_{\geq 0} \to \mathbb{R}^m$: perception fields.
- $x(t) \in \mathcal{X}$: latent state of Spatial AI.
- $\theta_i(t)$: oscillator phases; dynamic coherence.
- $\varepsilon(u)$, ε^{eig}: elastic strain and eigenstrain.
- $C_{\text{eff}}, \kappa_{\text{eff}}$: effective elasticity and conductivity.

- $\mathrm{CS}, \mathrm{CD}, \mathrm{CI}_{\mathrm{int}}, \mathrm{CI}$: coherence functionals.
- Φ: perfect attractor potential; coherence field.
- $\beta(I)$: Betti vector of overlap complex; computon state.
- μ_i, Σ_i: local beliefs in WGC Gaussian nodes.

We use $\langle \cdot, \cdot \rangle$ for Euclidean inner products, $\| \cdot \|$ for corresponding norms, and L to denote graph Laplacians.

3 Perception Fields and State Geometry

Let $X \subset \mathbb{R}^d$ denote the spatial domain of the environment. Time $t \geq 0$.

Definition 3.1 (Perception Field)**.** A perception field is a measurable map

$$\phi : X \times \mathbb{R}_{\geq 0} \to \mathbb{R}^m,$$

encoding multimodal environmental sensing.

Examples include:

- acoustic intensity and phase,
- heat and thermal gradients,
- EM signal strength and phase,
- motion density, occupancy,
- semantic occupancy fields (e.g., probability of human presence).

The environment maintains an internal representation

$$x(t) \in \mathcal{X},$$

where $\mathcal{X}$ is a manifold or high-dimensional latent space that collects a compressed yet expressive description of the environment's state.

4 Coherence Axes

We define three independent forms of coherence and then aggregate them into a single order parameter.

4.1 Structural Coherence

Let $G = (V, E)$ be the node interaction graph, x_i the state associated with node i.

$$E_{\text{str}}(x) = \frac{1}{2} \sum_{(i,j)\in E} w_{ij} \|x_i - x_j\|^2.$$

Define the structural coherence

$$\text{CS}(x) = 1 - \frac{E_{\text{str}}(x)}{E_{\max}},$$

where $E_{\max}$ is an a priori or empirical upper bound.

High CS corresponds to smoothness of x over the graph geometry.

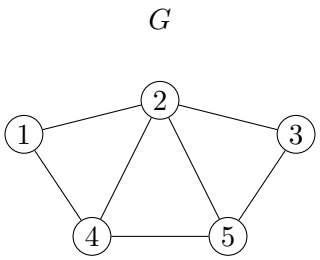

Figure 2: Example interaction graph G used to define structural energy and coherence CS.

4.2 Dynamic Coherence

Let each node have a phase $\theta_i(t)$ (oscillator or update phase). Define

$$\text{CD}(x) = \left| \frac{1}{N} \sum_{i=1}^{N} e^{i\theta_i} \right|.$$

This is the classic Kuramoto order parameter: CD = 1 for perfect phase alignment, and CD ≈ 0 for desynchronized states.

In non-oscillatory settings, dynamic coherence can be defined via velocity covariance or direction alignment metrics.

4.3 Intent Coherence

Let $U(x)$ be a local cost functional and $\Phi(x)$ an attractor potential. For coupling strength $\alpha \geq 0$ define the effective potential:

$$V_\alpha(x) = U(x) - \alpha\Phi(x).$$

Intent coherence measures how close the system is to a joint optimum of task performance and attractor alignment:

$$\mathrm{CI}_{\mathrm{int}}(x) = 1 - \frac{\|\nabla V_\alpha(x)\|}{C_{\mathrm{int}}},$$

for some scaling constant $C_{\mathrm{int}} > 0$.

4.4 Unified Coherence Index

We aggregate the axes into a single order parameter:

$$\mathrm{CI}(x) = w_S\,\mathrm{CS}(x) + w_D\,\mathrm{CD}(x) + w_I\,\mathrm{CI}_{\mathrm{int}}(x), \quad w_S, w_D, w_I \geq 0,\ w_S + w_D + w_I = 1.$$

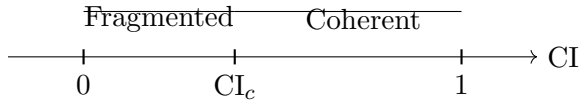

Figure 3: Coherence index CI as an order parameter with critical value CI_c.

5 Perfect Attractor Geometry

Let $c \in \mathbb{R}^d$ denote an attractor center. Let Q be a positive–definite anisotropy matrix.

Definition 5.1 (Perfect Attractor)**.** For nodes with positions $x_i \in \mathbb{R}^d$, define

$$\Phi(x) = \lambda \sum_{i=1}^{N} \frac{1}{(x_i - c)^\top Q (x_i - c)},$$

with scale $\lambda > 0$.

This is an anisotropic $1/r^2$-like potential that extends over the entire environment and encodes preferred coherence basins.

The gradient becomes

$$\nabla_{x_i}\Phi(x) = -2\lambda \frac{Q(x_i - c)}{\left((x_i - c)^\top Q(x_i - c)\right)^2}.$$

The attractor term in PCA dynamics,

$$\alpha \nabla \Phi(x),$$

acts as a long-range field pulling states into geometrically and intentionally coherent basins.

5.1 Visualizing the Attractor Field

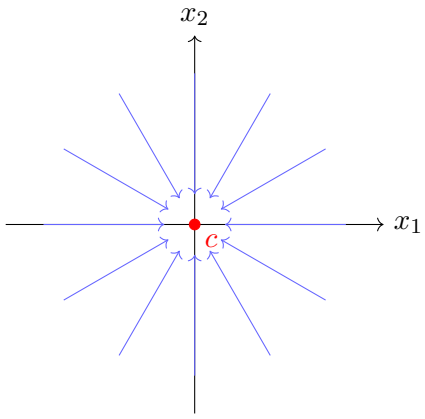

Figure 4: Schematic 2D slice of an isotropic perfect attractor field. Arrows show gradient direction $\nabla\Phi$ pointing toward the attractor center c.

6 Attractor–Driven Dynamics and Stability

We model system evolution as

$$\dot{x} = -\nabla U(x) + \alpha \nabla \Phi(x) - \beta L_{\text{dyn}} x + \sigma \eta(t),$$

where:

- $U(x)$: local performance cost (task, comfort, efficiency),
- $\Phi(x)$: perfect attractor potential,
- L_{dyn}: dynamic Laplacian (diffusive coupling),
- $\alpha, \beta, \sigma \geq 0$: scalar gains,
- $\eta(t)$: noise or exogenous disturbance.

Under suitable conditions $V_\alpha(x) = U(x) - \alpha\Phi(x)$ becomes a Lyapunov functional, ensuring convergence to a set of identity-consistent attractor states.

7 Oscillator Networks and Synchronization

Spatial AI often uses coupled oscillators (timing loops, rhythmic attention, communication slots). Let phases evolve as

$$\dot{\theta}_i = \omega_i + \sum_j K_{ij} \sin(\theta_j - \theta_i) + \alpha \frac{\partial \Phi}{\partial \theta_i}.$$

Define coherence

$$r(t) = \left| \frac{1}{N} \sum_{i=1}^{N} e^{i\theta_i(t)} \right|,$$

and note that the attractor term $\alpha \partial\Phi/\partial\theta_i$ lowers the critical coupling required for synchronization, effectively using intent to tighten dynamic coherence.

8 Tessellated Field Synthesis (TFS)

Tessellated Field Synthesis (TFS) provides programmable coherence in matter via eigenstrain-engineered transport tensors.

8.1 Domain and Mechanical Fields

Let $\Omega \subset \mathbb{R}^3$ be a bounded solid body.

At each $x \in \Omega$:

$$u(x,t) \in \mathbb{R}^3 \quad \text{(displacement field)}.$$

Define infinitesimal strain

$$\varepsilon(u) = \frac{1}{2}\left(\nabla u + \nabla u^\top\right).$$

Let

$$\varepsilon^{\text{eig}}(x)$$

be a locked-in eigenstrain.

Total strain

$$\varepsilon_{\text{total}} = \varepsilon(u) + \varepsilon^{\text{eig}}.$$

8.2 Constitutive Coupling

Let $C_{\text{eff}}(x)$ be the effective elasticity tensor and $\kappa_{\text{eff}}(x)$ the effective thermal conductivity. We assume

$$C_{\text{eff}} = C_0 + \mathcal{H}_C(\varepsilon^{\text{eig}}), \quad \kappa_{\text{eff}} = \kappa_0 + \mathcal{H}_\kappa(\varepsilon^{\text{eig}}),$$

where $\mathcal{H}_C$ and $\mathcal{H}_\kappa$ encode nonlinear strain–transport coupling, learned or characterized from microstructure.

A quadratic expansion yields

$$C_{\text{eff}} = C_0 + D :: \varepsilon^{\text{eig}} + \varepsilon^{\text{eig}} :: E :: \varepsilon^{\text{eig}},$$

and similarly for κ_{eff}.

8.3 Transport and Wave Equations

Heat transport:

$$c(x)\partial_t T = \nabla \cdot (\kappa_{\text{eff}} \nabla T).$$

Elastic/acoustic waves:

$$\rho \ddot{u} = \nabla \cdot (C_{\text{eff}} : \varepsilon(u)).$$

8.4 Metric Interpretation

Heat rays follow geodesics of

$$g_{ij} = (\kappa_{\text{eff}}^{-1})_{ij},$$

stress-wave geodesics follow

$$h_{ij} = (C_{\text{eff}}^{-1})_{ij}.$$

Thus eigenstrain defines geometry: by programming ε^{eig}, Spatial AI can sculpt effective metrics for thermal and mechanical transport.

8.5 Tessellations

Partition

$$\Omega = \cup_{i=1}^{N} \Omega_i$$

and assign material states

$$\zeta(x) \in \{1, \ldots, M\}.$$

Define free energy

$$\mathcal{F} = \int_{\Omega} \left(V(\zeta) + \frac{\beta}{2} |\nabla \zeta|^2 \right) dx.$$

Dynamics:

$$\partial_t \zeta = -\Gamma \frac{\delta \mathcal{F}}{\delta \zeta}.$$

8.6 Writing Eigenstrain

Let $\phi(x,t)$ denote a writer field (e.g., thermal, EM, mechanical). Switch tessellation states when

$$|\phi(x,t)| > \phi_{\text{thresh}}.$$

In this way, Spatial AI can slowly rewrite the routing geometry without continuous power.

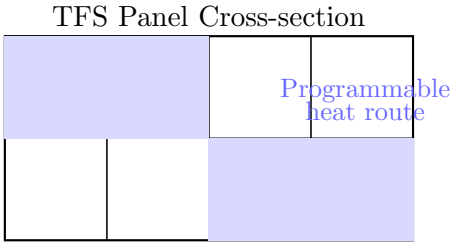

Figure 5: Schematic TFS panel with tessellated eigenstrain-programmable cells defining a preferred heat or acoustic route.

9 Whisper Graph Communication (WGC)

Whisper Graph Communication (WGC) is a probabilistic communication layer in which nodes exchange noisy "whispers" of their internal beliefs rather than exact messages. It is designed to be low-power, privacy-preserving, and naturally compatible with coherence-oriented control.

9.1 Gaussian Beliefs on a Graph

Let $G = (V, E)$ be a connected undirected graph with $N = |V|$ nodes. Each node $i \in V$ maintains a Gaussian belief over some latent quantity $z \in \mathbb{R}^k$:

$$p_i(z) = \mathcal{N}(z; \mu_i, \Sigma_i),$$

where $\mu_i \in \mathbb{R}^k$ and $\Sigma_i \in \mathbb{R}^{k \times k}$ is symmetric positive definite.

At time t, a node emits a whisper

$$y_i(t) = \mu_i(t) + \varepsilon_i(t), \quad \varepsilon_i(t) \sim \mathcal{N}(0, \sigma_i^2 I),$$

toward its neighbors. The whisper is thus a noisy sample of its current best estimate.

We denote by $\mathcal{N}(i)$ the neighborhood of node i.

9.2 Whisper Update Rule

At each discrete step (or slow continuous-time limit), node i updates its mean belief using its previous mean and the whispers it receives:

$$\mu_i(t+1) = (1-\alpha_i)\mu_i(t) + \alpha_i \sum_{j\in\mathcal{N}(i)} w_{ij}\, y_j(t),$$

with $w_{ij} \geq 0$, $\sum_{j\in\mathcal{N}(i)} w_{ij} = 1$, and $0 < \alpha_i \leq 1$. In matrix form, for the stacked mean vector $\mu(t) \in \mathbb{R}^{Nk}$, this is

$$\mu(t+1) = A\mu(t) + \varepsilon(t),$$

where A is a row-stochastic matrix derived from (α_i, w_{ij}) and $\varepsilon(t)$ aggregates the whisper noise.

A simple choice is

$$A = (1-\alpha)I + \alpha W, \quad 0 < \alpha \leq 1,$$

where W is a symmetric stochastic matrix with $W_{ij} > 0$ only on edges $(i,j) \in E$.

9.3 Whisper Graph as a Stochastic Kernel

We can interpret W as a transition kernel of a random walk on G. The whisper update is then a convex combination of self-belief and a random-walk averaging step. For $0 < \alpha < 1$, the operator A satisfies:

$$A = I - \alpha(I - W) = I - \alpha L_W,$$

where $L_W = I - W$ is a random-walk Laplacian.

If G is connected and W is irreducible and aperiodic, then A is primitive and its largest eigenvalue is $\lambda_1(A) = 1$ with multiplicity one. All other eigenvalues satisfy $|\lambda_i(A)| < 1$.

Theorem 9.1 (Mean Consensus under WGC)**.** *Assume G is connected, W is symmetric and stochastic, and $0 < \alpha \leq 1$. If the whisper noise has zero mean, $\mathbb{E}[\varepsilon(t)] = 0$, then*

$$\mathbb{E}[\mu(t)] \to \bar{\mu}\mathbf{1},$$

where

$$\bar{\mu} = \frac{1}{N} \sum_{i=1}^{N} \mu_i(0),$$

and $\mathbf{1}$ *is the all-ones vector. Moreover, the convergence rate is controlled by the spectral gap* $1 - \lambda_2(A)$*.*

Proof. Standard stochastic consensus analysis: since A is row-stochastic, $\mathbf{1}$ is a right eigenvector with eigenvalue 1. Symmetry of W implies $\bar{\mu}\mathbf{1}$ is an invariant subspace. Connectedness ensures that 1 is a simple eigenvalue and all others are strictly inside the unit circle, so $A^t \to \mathbf{1}\pi^\top$ where π is the stationary distribution. For symmetric W, π is uniform. Taking expectations and using $\mathbb{E}[\varepsilon(t)] = 0$ yields the consensus limit. □

9.4 Information-Theoretic Whisper Coherence

We define an information-theoretic whisper coherence metric using the variance of node means around their global average.

Let

$$\bar{\mu}(t) = \frac{1}{N} \sum_{i=1}^{N} \mu_i(t),$$

and define the average squared deviation

$$\mathcal{V}(t) = \frac{1}{N} \sum_{i=1}^{N} \|\mu_i(t) - \bar{\mu}(t)\|^2.$$

We can then define a normalized WGC coherence

$$C_{\text{wgc}}(t) = 1 - \frac{\sqrt{\mathcal{V}(t)}}{\sigma_{\text{ref}}},$$

where σ_{ref} is a reference scale, e.g. based on prior uncertainty.

Proposition 9.2. *In the noise-free case* ($\varepsilon = 0$) *with connected* G *and stochastic* W*, we have* $\mathcal{V}(t) \to 0$*, hence* $C_{\text{wgc}}(t) \to 1$*.*

In the noisy case, $\mathcal{V}(t)$ converges to a noise floor that scales with the magnitude of $\varepsilon(t)$ and the spectral gap of A.

9.5 Whisper Graph TikZ Diagram

WGC Whisper Graph

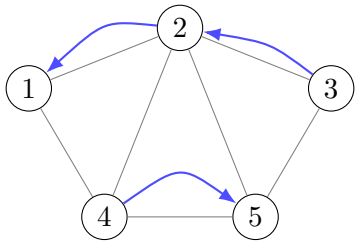

Figure 6: Whisper Graph Communication: nodes exchange noisy belief whispers along edges of G, gradually reaching probabilistic consensus.

9.6 Integration of WGC with Coherence and Attractors

In Spatial AI, WGC is not just a communication protocol; it is coupled to coherence and attractor dynamics:

- CI can be extended to include C_{wgc} as an additional axis for communication coherence.
- Attractor fields Φ can be used to modulate α_i or w_{ij}, biasing whisper flow along coherent pathways.
- WGC can implement probabilistic voting for LCF mode switches, where computon states determine which attractor wells are active.

We can define an extended coherence index

$$\text{CI}_{\text{ext}} = w_S\,\text{CS} + w_D\,\text{CD} + w_I\,\text{CI}_{\text{int}} + w_W C_{\text{wgc}},$$

with $w_W \geq 0$ and updated normalization.

10 Homogenization Theory for TFS

Introduce microscale variable $y = x/\epsilon$.

Cell problem

$$\nabla_y \cdot (C(y,\zeta) : \nabla_y w_{mn}) = 0,$$

yielding

$$C_{\text{eff}}^{ijkl} = \int_Y C^{pqrs} \left(\delta_{ip}\delta_{jq} + \partial_{y_p} w_{ij}^q\right) (\delta_{kr}\delta_{ls} + \partial_{y_r} w_{kl}^s)\, dy.$$

This determines macroscale routing geometry from tessellated microstructure.

11 Inverse Design and Optimization

Let u solve PDE

$$\mathcal{P}(u;\zeta) = 0.$$

Define cost

$$J(\zeta) = \int_\Omega L(x,u)\, dx + R(\zeta),$$

and solve

$$\min_{\zeta \in \mathcal{A}} J(\zeta)$$

subject to PDE constraints.

11.1 Protected Region Example

Let $D \subset \Omega$.

Acoustic energy density

$$E_a = \frac{1}{2}\left(\rho|\dot{u}|^2 + \varepsilon : C_{\text{eff}} : \varepsilon\right).$$

Objective

$$J = \int_D E_a\, dx + \lambda \int_\Omega |\nabla\zeta|^2 dx.$$

We design material routing to silence D.

11.2 Simulation Pipeline

1. Mesh Ω.

2. Assign ζ_i.

3. Compute C_{eff} and κ_{eff}.

4. Solve PDEs for u, T.

5. Evaluate J.

6. Update ζ via simulated annealing or topology optimization.

7. Repeat until convergence.

12 Lattice of Computable Fields (LCF)

LCF provides the logical engine of Spatial AI, using field overlaps and topology instead of discrete wires and gates.

Let field family $F = \{F_i\}$ with overlap region

$$I(F) = \bigcap_i \text{supp}(F_i).$$

Homology yields a Betti vector

$$\beta(I) = (\beta_0, \beta_1, \dots),$$

called the **computon**. Computon types form elements of a lattice, ordered by refinement and local constructibility.

Computon braiding in space–time defines logic: transitions between computon types, and their worldline linkings, implement discrete operations that are robust to local perturbations.

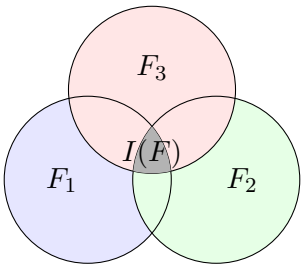

Figure 7: Schematic of a triple-overlap region $I(F)$ whose homology yields a computon state.

12.1 LCF as a Lattice (TikZ Hasse Diagram)

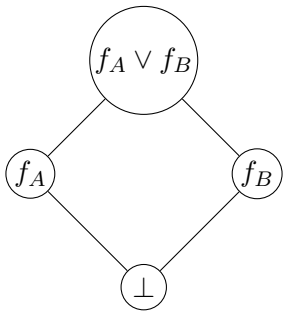

Figure 8: Toy Hasse diagram of part of the lattice $\mathcal{L}$ of computable fields, with bottom element $\bot$ and join $f_A \vee f_B$.

13 Spatial AI as Unified System

Collecting the components, Spatial AI is the coupled evolution of

$$(\phi(t), x(t), \theta(t), \varepsilon^{\text{eig}}(t), \beta(I(t)), \mu(t)),$$

with feedback through coherence, attractors, TFS geometry, WGC belief flow, and LCF logic.

14 Closed–Loop Diagram

15 Lyapunov Stability and Identity Attractors

Let Φ denote the space of perception fields with norm $\|\cdot\|_{L^2(X)}$. Let $\mathcal{A} \subset \Phi$ denote the set of identity–consistent fields.

Definition 15.1 (Identity Attractor)**.** A set $\mathcal{A} \subset \Phi$ is an *identity attractor* if

1. it is forward invariant under the system dynamics, and
2. there exists an open neighborhood U such that for any $\phi_0 \in U$, the solution $\phi(t)$ satisfies

$$\text{dist}(\phi(t), \mathcal{A}) \to 0 \quad \text{as} \quad t \to \infty.$$

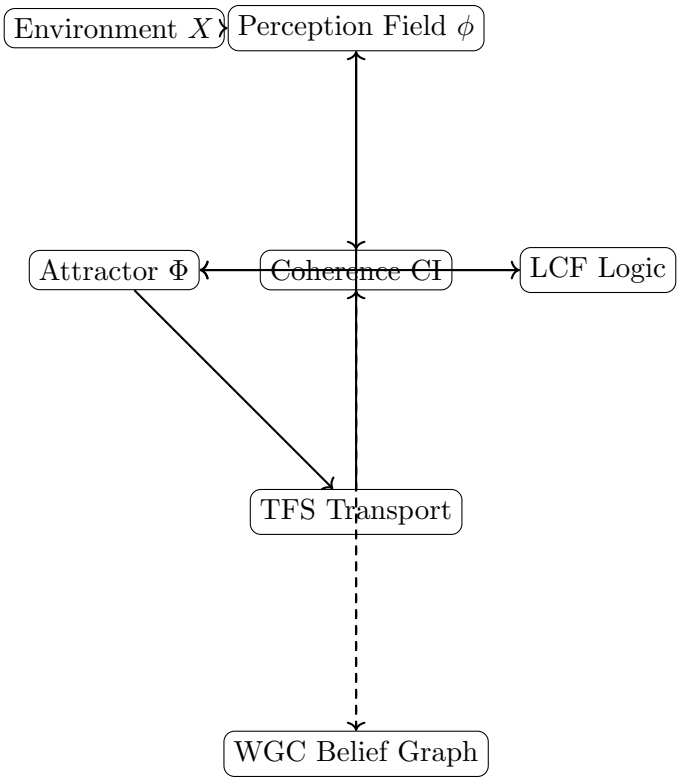

Figure 9: Closed–loop Spatial AI with TFS, WGC, and LCF.

Theorem 15.2 (Lyapunov Stability of Spatial Identity)**.** *Suppose there exists a functional* $V : \Phi \to \mathbb{R}_{\geq 0}$ *such that:*

1. $V(\phi) = 0$ *iff* $\phi \in \mathcal{A}$,
2. $V(\phi) > 0$ *otherwise,*
3. *along trajectories of* $\phi(t)$,

$$\frac{d}{dt} V(\phi(t)) \leq -\gamma \, \|\phi(t) - \Pi_{\mathcal{A}} \phi(t)\|^2,$$

for some $\gamma > 0$*, where* $\Pi_{\mathcal{A}}$ *denotes projection.*

Then $\mathcal{A}$ *is globally asymptotically stable.*

16 Spectral Phase Transitions in Coherence

Linearizing PCA dynamics near equilibrium gives

$$\dot{y} = -H_U y + \alpha H_\Phi y - \beta L_{\text{dyn}} y,$$

where H_U and H_Φ are Hessians.

Definition 16.1 (Effective Stability Operator)**.**

$$\mathcal{L}_\alpha = H_U - \alpha H_\Phi + \beta L_{\text{dyn}}.$$

Theorem 16.2 (Spectral Coherence Transition)**.** *Let $\lambda_{\min}(\mathcal{L}_\alpha)$ denote the smallest eigenvalue. If $\lambda_{\min}(\mathcal{L}_\alpha)$ crosses zero at $\alpha_c > 0$, then the system undergoes a coherence phase transition.*

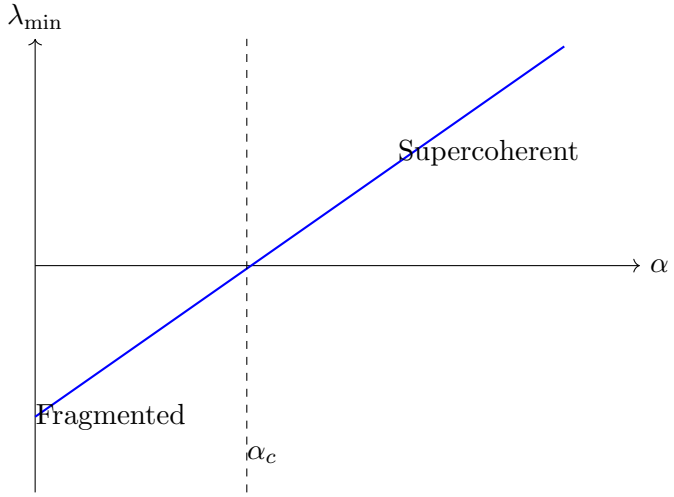

Figure 10: Spectral coherence threshold

17 Information–Theoretic Coherence

Let $p_\phi(x)$ be a normalized magnitude distribution of the field.

Entropy:

$$H(\phi) = -\int_X p_\phi(x) \log p_\phi(x)\, dx.$$

Let s denote sensor streams; then

$$I(\phi; s) = H(\phi) - H(\phi|s).$$

Definition 17.1 (Information Coherence)**.**

$$C_{\text{info}}(t) = \frac{I(\phi; s)}{H(\phi)}.$$

C_{info} is a statistically grounded anomaly metric: when the environment behaves in unmodeled ways, conditional entropy increases and information coherence drops.

18 Multiscale Coherence Formalism

Let $\mathcal{X}_0, \ldots, \mathcal{X}_L$ denote scale-spaces and $\Pi_{\ell+1,\ell}$ coarse-graining maps.

$$\text{CI}_{\text{global}} = \sum_{\ell=0}^{L} \gamma_\ell \left(w_{S,\ell}\, \text{CS}_\ell + w_{D,\ell}\, \text{CD}_\ell + w_{I,\ell}\, \text{CI}_{\text{int}\ \ell} \right).$$

This allows coherence to propagate upward in scale and to be monitored at coarse-grained levels (e.g., room, floor, building).

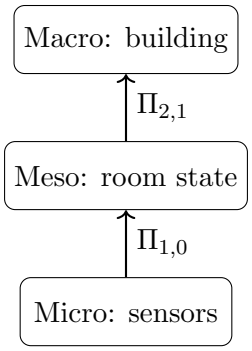

Figure 11: Multiscale hierarchy for Spatial AI coherence.

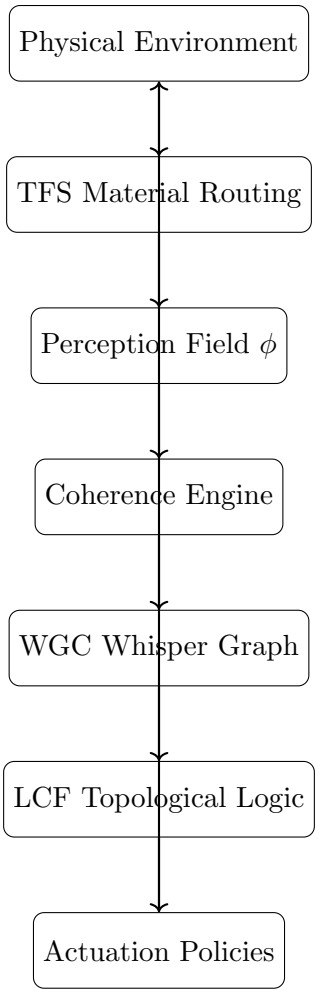

Figure 12: Spatial AI Engineering Stack

19 Engineering Stack Architecture

20 Comparative Taxonomy of Architectures

21 Design Patterns and Reference Architectures

21.1 Quiet Room Pattern

- *Objective*: Maintain high speech intelligibility in a focus zone while suppressing external noise and cross-talk.
- *Mechanism*:
  - Perception fields capture acoustic pressure and direction.

Table 1: Spatial AI Implementation Layers

Layer	Role	Examples
P	Physical substrate	Walls, beams, ducts, seats, TFS-programmable panels
S	Sensing	Microphone arrays, thermal cameras, IMUs, strain gauges, RF receivers
F	Field representation	Acoustic maps, occupancy probability fields, EM intensity fields
C	Coherence and logic	PCA dynamics, attractor updates, LCF state machine, WGC consensus
A	Actuation	HVAC dampers, lights, speakers, motor drives, displays, haptics

  - Coherence index CI biases toward attractors representing "single speaker + low background" states.
  - TFS panels route and dissipate noise away from the focus zone.
  - WGC exchanges local noise estimates between panels to maintain probabilistic consensus on quiet zones.
  - LCF logic enforces topological invariants preventing self-exciting feedback loops.

21.2 Adaptive Corridor Pattern

- *Objective*: Maintain safe pedestrian flow and comfort in a long corridor under varying occupancy.
- *Mechanism*:
  - Occupancy fields and velocity fields form a dynamic perception layer.
  - Coherence penalizes spatial congestion and abrupt changes.
  - Attractor fields represent desired flow corridors.
  - WGC allows local clusters of sensors to whisper about density and update corridor-level flow beliefs.
  - TFS controls acoustic and thermal gradients to discourage bottlenecks.

Table 2: Comparison of Architectural Paradigms

Dimension	Centralized Cloud AI	Edge/IoT System	Spatial AI
Primary substrate	Datacenter compute	Devices and gateways	Physical environment + fields
State representation	Data streams, models	Device variables	Coherent fields + topology
Coordination	Network protocols	Local rules + cloud	Attractor fields + coherence + WGC
Robustness	Network-dependent	Device-level redundancy	Geometric, topological, and probabilistic
Computation locus	Remote servers	Edge devices	Distributed fields (LCF)
Physical integration	Weak	Moderate	Strong, geometry-coded

21.3 Vehicle Cabin Pattern

- *Objective*: Provide coherent audio, lighting, and thermal comfort, while respecting safety and energy constraints.
- *Mechanism*:
  - Cabin perception fields capture sound, motion, and occupancy.
  - Coherence enforces consistent experience across seats.
  - WGC fuses seat-local preferences into a global comfort belief.
  - LCF ensures emergency mode logic is topologically protected from regular UI flows.
  - TFS (structural) is used for passive acoustic shaping and vibration control in panels.

22 Implementation Considerations

22.1 Sensing and Bandwidth

Spatial AI must balance:

- spatial resolution of fields,
- temporal sampling,

- onboard compute budgets,
- privacy and security.

Field representations may be compressed into low-dimensional latent bases, graph wavelets, or learned basis functions; PCA coherence metrics act on these compressed representations.

22.2 Computation and Deployment

The coherence engine, WGC, and LCF logic may be implemented on:

- embedded CPUs with GPU accelerators,
- neuromorphic chips for oscillator and spiking dynamics,
- FPGAs for TFS writer control loops.

22.3 Privacy and Observability

Because perception fields and beliefs can be high-dimensional, the architecture should:

- minimize direct storage of raw data, favoring field statistics, belief summaries, and coherence metrics,
- provide local interpretability channels (e.g., coherent overlays of CI and C_{wgc} on spatial maps),
- support audit of LCF mode transitions and attractor selection.

23 Use-Case Scenarios

23.1 Spatial AI Room

A conference room with:

- ceiling microphone arrays and speakers,
- controllable HVAC and lighting,
- optional TFS acoustic panels,

- WGC whisper meshes between smart tiles.

Spatial AI maintains coherent speech zones, comfortable thermal fields, and low-noise backgrounds, while enforcing safety constraints and supporting topological invariants such as guaranteed emergency alert paths.

23.2 Spatial AI Factory Cell

An industrial cell with:

- vibration and load perception fields,
- TFS routing of stress away from sensitive components,
- WGC coordination among machines about load and anomaly beliefs,
- LCF invariants encoding safety constraints (e.g., intrusion zones).

Anomalies are detected via drops in CI, C_{info}, and C_{wgc}, triggering mode switches and safe shutdowns.

23.3 Spatial AI Vehicle Cabin

A vehicle cabin with:

- audio, occupancy, and motion perception fields,
- TFS-based passive acoustic shaping,
- active Spatial AI control of audio, lighting, and haptics,
- WGC-based passenger comfort and intent aggregation.

Emergency modes are LCF-coded, guaranteeing that certain topological corridors for alerts remain intact.

24 Ethics, Safety, and Governance

Spatial AI requires governance principles:

- transparency of environmental behavior to occupants,
- bounded actuation and clear physical limits,
- local override and fail–safe behavior independent of network,
- auditability of LCF logic and WGC belief dynamics,
- physical safety margins in TFS routing and attractor design.

25 Roadmap

1. Demonstrate stable identity fields in simple rooms.
2. Validate coherence phase transitions in oscillator arrays.
3. Implement basic LCF computon gates on field overlaps.
4. Build TFS prototypes for routing heat and sound.
5. Deploy WGC whisper meshes on small device graphs.
6. Integrate full Spatial AI stack in pilot environments and evaluate coherence metrics, energy budgets, and human comfort.

26 Conclusion

We have developed a unified theoretical and engineering architecture for Spatial AI integrating: coherence theory, attractor geometry, programmable transport in matter, whisper-based probabilistic communication, and topological computation.

Environments become coherent, intelligent spaces—not just hosts for devices, but agents with identity, memory, and mode structure encoded directly in their geometry, fields, and whisper graphs. The path from theory to deployed systems runs through careful metric design, material engineering,

probabilistic protocol design, and topology-aware safety constraints, all of which are now available as explicit mathematical objects within this framework.

A.1 Appendix A: Mathematical Foundations and Proofs

A.1.1 Structural Coherence as Dirichlet Energy

Let $G = (V, E)$ be a connected, undirected weighted graph with Laplacian L. Define structural energy

$$E_{\text{str}}(x) = \frac{1}{2} \sum_{(i,j)\in E} w_{ij} \|x_i - x_j\|^2.$$

Theorem A.1.1. *$E_{\text{str}}(x) = 0$ iff x is constant on every connected component.*

Proof. Immediate from $w_{ij} > 0$ and $\|x_i - x_j\|^2 = 0 \iff x_i = x_j$. □

Thus $\text{CS}(x) = 1$ characterizes consensus.

A.1.2 Coherence Index as Order Parameter

Let

$$\text{CI}(x) = w_S \,\text{CS} + w_D \,\text{CD} + w_I \,\text{CI}_{\text{int}} \,.$$

Theorem A.1.2. *If each component is continuous in x, then* CI *is continuous.*

Proof. Linear combination of continuous functionals. □

Phase transitions correspond to non-analytic behavior of emergent dynamics, not the index itself.

A.2 Appendix B: Spectral Coherence Thresholds

Consider linearized PCA dynamics

$$\dot{y} = -\left(H_U - \alpha H_\Phi + \beta L\right) y.$$

Define effective operator

$$\mathcal{L}_\alpha = H_U - \alpha H_\Phi + \beta L.$$

Theorem A.2.1. *Let $\lambda_{\min}(\mathcal{L}_\alpha)$ be the smallest eigenvalue. A coherence transition occurs when*

$$\lambda_{\min}(\mathcal{L}_{\alpha_c}) = 0.$$

Proof. Zero crossing implies change of stability sign in dominant eigenmode. □

A.3 Appendix C: Kuramoto–Attractor Hybrid Analysis

Kuramoto–PCA model

$$\dot{\phi}_i = \omega_i + \frac{K}{N}\sum_j a_{ij}\sin(\phi_j - \phi_i) + \alpha\frac{\partial \Phi}{\partial \phi_i}.$$

Define order parameter

$$Re^{i\psi} = \frac{1}{N}\sum_j e^{i\phi_j}.$$

Under mild symmetry,

$$\dot{\phi}_i = \omega_i + KR\sin(\psi - \phi_i) + \alpha G(\phi_i).$$

If $\alpha > 0$ sharpens curvature of the potential landscape, then the critical coupling satisfies

$$K_c(\alpha) < K_c(0).$$

A.4 Appendix D: Mechanics of TFS Eigenstrain Routing

Total strain:

$$\varepsilon_{\text{total}} = \varepsilon(u) + \varepsilon^{\text{eig}}.$$

Stress:

$$\sigma = C_{\text{eff}} : \varepsilon_{\text{total}}.$$

Static equilibrium:

$$\nabla \cdot \sigma = 0.$$

Residual stress $\sigma^\star = C_{\text{eff}} : \varepsilon^{\text{eig}}$ produces no net force iff

$$\nabla \cdot \sigma^\star = 0.$$

A.5 Appendix E: Numerical Schemes

A.5.1 Finite Element Solution Strategy

1. Discretize Ω into tetrahedral mesh.

2. Assemble stiffness matrix
$$K = \int_\Omega B^\top C_{\text{eff}} B \, dx.$$

3. Apply boundary conditions.

4. Solve
$$Ku = f.$$

5. Compute energy
$$E = \frac{1}{2} u^\top K u.$$

A.5.2 Topology Optimization Loop

1. Initialize ζ.

2. Solve PDEs.

3. Compute sensitivity
$$\frac{\partial J}{\partial \zeta_i}.$$

4. Apply regularization.

5. Threshold update rule.

6. Repeat until convergence.

A.6 Appendix F: Lattice of Computable Fields (LCF)

Definition A.6.1 (Computable Field)**.** A computable field is a map

$$f : \Omega \to \mathbb{R}^n$$

such that its evaluation and update laws are locally realizable in spatial media.

Definition A.6.2 (Lattice of Computable Fields)**.** Define a partially ordered set

$$\mathcal{L} = \{f_i\}$$

with order relation

$$f_i \preceq f_j \iff f_j \text{ can be constructed from } f_i \text{ by local operators.}$$

Theorem A.6.3. $(\mathcal{L}, \preceq)$ *forms a lattice.*

A.7 Appendix G: Toy 1D Spatial AI Model

Consider a 1D domain $X = [0, 1]$ with scalar field $\phi(x, t)$. Let

$$\partial_t \phi = D\partial_{xx}\phi - \partial_\phi U(\phi) + \alpha \partial_\phi \Phi(\phi),$$

with $D > 0$ and simple potentials, e.g.

$$U(\phi) = \frac{a}{4}(\phi^2 - 1)^2, \quad \Phi(\phi) = b\phi.$$

Then coherence corresponds to alignment of ϕ toward ± 1, biased by b. This toy system illustrates how Spatial AI can implement bistable modes biased by attractor fields.

A.8 Appendix H: WGC Noise Floor and Spectral Gap

In discrete-time WGC with symmetric stochastic W and $A = (1-\alpha)I + \alpha W$, the covariance of $\mu(t)$ around the consensus direction can be analyzed via the eigen-decomposition of A.

Let $A = Q\Lambda Q^\top$ with eigenvalues $1 = \lambda_1 > \lambda_2 \geq \cdots \geq \lambda_N > -1$ and orthonormal Q. Decompose $\mu(t) - \bar{\mu}\mathbf{1} = Q\tilde{\mu}(t)$ in this basis. The non-consensus modes evolve as

$$\tilde{\mu}_i(t+1) = \lambda_i \tilde{\mu}_i(t) + \tilde{\varepsilon}_i(t), \quad i \geq 2.$$

Assuming $\varepsilon(t)$ is white with covariance Σ_ε, each mode has steady-state variance

$$\mathrm{Var}(\tilde{\mu}_i) \approx \frac{\Sigma_{\varepsilon,i}}{1-\lambda_i^2}.$$

Thus the noise floor is controlled by the spectral gap $1 - \max_{i\geq 2}|\lambda_i|$. Faster-mixing graphs (larger gap) yield lower steady-state WGC variance for a fixed noise level.

A.9 Appendix I: Example Scales and Parameters

Approximate design ranges:

- Room-scale Spatial AI: X on the order of 10^1–10^2 m^2.
- TFS panels: Ω thickness $\sim$ cm, lateral size $\sim$ m.
- Perception update rates: 10–200 Hz, depending on modality.
- Coherence control rates: 1–10 Hz for macroscopic attractor updates.
- TFS reprogramming: seconds to minutes, treated as quasi-static.
- WGC update intervals: 0.1–10 s, depending on graph size and energy budget.

A.10 Glossary of Key Terms

- **Structural Coherence** — smoothness of state across graph.

- **Dynamic Coherence** — temporal/phase alignment.
- **Intent Coherence** — alignment to attractor field.
- **Perfect Attractor** — long-range coherence basin.
- **TFS** — strain-programmed transport routing.
- **WGC** — whisper-based probabilistic consensus on graphs.
- **LCF** — topology of computable spatial fields.
- **Spatial AI** — cognition embedded in matter + fields.

A.11 References

References

[1] Y. Kuramoto, *Chemical Oscillations, Waves, and Turbulence*. Springer, 1984.

[2] L. Landau and E. Lifshitz, *Theory of Elasticity*. Butterworth-Heinemann, 1986.

[3] N. Engheta, *Metamaterials: Physics and Engineering Explorations*. Wiley, 2006.

[4] S. Torquato, *Random Heterogeneous Materials*. Springer, 2001.

[5] M. Bendsoe and O. Sigmund, *Topology Optimization*. Springer, 2003.

[6] R. Olfati-Saber, J. Fax, and R. Murray, *Consensus and cooperation in networked multi-agent systems*. Proceedings of the IEEE, 95(1), 2007.